Int. J. Heat Mass Transfer. Vol. 36, No. 15, pp. 3813–3822, 1993
Printed in Great Britain

0017–9310/93 $6.00 + 0.00

Analysis of critical and subcritical flow boiling

R. W. LYCZKOWSKI,† H. M. DOMANUS,‡ M. BOTTONI‡ and W. T. SHA‡

† Energy Systems Division and ‡ Materials & Components Technology Division,
Argonne National Laboratory, 9700 South Cass Avenue, Argonne, IL 60439, U.S.A.

(*Received* 10 *January* 1992 *and in final form* 23 *February* 1993)

Abstract—Low pressure flow boiling has been computer-simulated by means of the Homogeneous Equilibrium Mixture (HEM) and algebraic slip model of two-phase flow using a transient computer code. Numerical difficulties were experienced when the two-phase velocity exceeded the HEM model's speed of sound at the inception of boiling during the solution procedure. An apparent anomaly experienced was the calculation of pressure undershoots ('kinks') across a two-phase boiling region surrounded by single-phase subcooled liquid. It is clearly shown that the HEM model's speed of sound is a critical state for the evaluation of the pressure gradient. When this speed of sound is not exceeded at the inception of boiling, numerically stable and accurate results are computed. Some means of resolving these apparently fundamental and generic problems are suggested.

1. INTRODUCTION

IN CONTRAST to high-pressure boiling (usually referred to as flashing), such as that occurring during piping breaks in pressurized or boiling water reactors (PWRs or BWRs), boiling of sodium near atmospheric pressure occurs during upsets (e.g. pump failures) in liquid metal fast reactors. The analysis of this low-pressure forced convection or flow boiling using transient numerical methods proves to be very difficult. One reason for this difficulty is that as the flow is decreased, the pressure drop begins to rise as boiling begins. The result is the well-known 'S'-shaped relationship between pressure drop and flow. This can lead to boiling instabilities.

Another, more serious difficulty encountered during the analysis of the steady-state sodium flow boiling experiments of Savatteri and Kottowski [1] using the transient two-phase COMMIX-2 computer code [2] was the possibility that the velocity of the two-phase mixture at the initiation of boiling could exceed the Homogeneous Equilibrium Mixture (HEM) model speed of sound. When this occurs, numerical instability usually results.

The major purpose of this paper is to present the results of an investigation into the source of the numerical instability by analyzing a one-dimensional model of a steady-state flow boiling experiment used as a benchmark problem of the European Liquid Metal Boiling Working Group [3]. Another objective is to present several related analyses and simulations that serve to diagnose the reason for the instability. The primary difficulty appears to involve the proper numerical treatment of 'internal choking' (i.e. critical flow that occurs away from breaks or area changes). Another, less serious difficulty involves the momentum–flux formulation in the vicinity of large density changes.

It is conclusively demonstrated that (1) the HEM speed of sound is a critical state for the pressure gradient calculation and (2) the numerical instability disappears when the HEM speed of sound is not exceeded. None of the slip models used in this study destabilizes the results in this case. Now that this apparently fundamental modeling problem has been identified, suggestions for its resolution are solicited.

2. STEADY-STATE SODIUM FLOW BOILING SIMULATIONS

The steady-state low-pressure sodium flow boiling experiments of Savatteri and Kottowski [1] were performed in order to obtain definitive pressure drop vs flow rate data in simple, well-defined geometries. They were performed using round and annular flow channels. One of the round tube tests was chosen for simulation. The details of the experimental setup are described in ref. [1] and are briefly summarized herein. The internal diameter of the round tube was 6 mm, and the heated length was 1 m. A condenser mounted some distance above an unheated region was kept at a cover gas pressure of 0.8 bar. In general, the boiling was initiated by decreasing the flow rate at constant heat flux. The inlet sodium temperature was maintained at 585 ± 15°C. The series of runs at 127 W cm^{-2} was chosen because of the largest number of measurements, 14 over the range of 0.5 to 5 m s^{-1}. Boiling was found to begin at 2.5 m s^{-1}. The reported nominal power level was 25 kW, but the actual power level has been determined to be 23.94 kW. The computer code used for the simulations is COMMIX-2 [2]. COMMIX-1A [4] has provided the basic structure for the development of two two-phase flow models, which are incorporated into COMMIX-2.

The first of these models is a three-equation slip model (SM), which provides for either a constant slip ratio or a relative velocity normalized by the mixture

NOMENCLATURE

a_h HEM model's speed of sound at constant enthalpy [m s^{-1}]
a_s HEM model's speed of sound at constant entropy [m s^{-1}]
D hydraulic diameter [m]
G mass flux [kg m^{-2} s^{-1}]
g acceleration due to gravity [m s^{-2}]
$\tilde{\mathbf{H}}$ slip ratio, $\tilde{\mathbf{v}}_g/\tilde{\mathbf{v}}_l$
h_m mixture enthalpy, $\alpha h_g+(1-\alpha)h_l$ [J kg^{-1}]
P pressure [Pa]
δP^{n+1} pressure increment, $P^{n+1}-P^n$ [Pa]
$\tilde{q}$ heat flux [W m^{-2}]
Q volumetric heat source [W m^{-3}]
Δt time-step size [s]
t time [s]
u, v, w components of velocity vector [m s^{-1}]
$\tilde{\mathbf{v}}$ velocity vector [m s^{-1}]
$\tilde{\mathbf{v}}_{SL}$ $\tilde{\mathbf{v}}_g-\tilde{\mathbf{v}}_l$, slip velocity vector [m s^{-1}]
$\tilde{\mathbf{v}}_{SL}^N$ normalized slip velocity, $\tilde{\mathbf{v}}_{SL}/\tilde{\mathbf{v}}_m$
x thermodynamic quality, $(h_m-h_l)/h_g-h_l)$.

Greek symbols
α void fraction, α_g
α_l $1-\alpha$
μ viscosity [Pa s]
ρ_m mixture density, $(\rho_g+(1-\alpha)\rho_l)$ [kg m^{-3}].

Subscripts and superscipts
g, l, m vapor, liquid, and coolant mixture, respectively
$k, k+1$ iteration indices at time step level $n+1$
$n, n+1$ discretization indices at times t and $t+\Delta t$.

velocity in each of the coordinate directions. The limiting case of equal phase velocities, known as the HEM model, is a subcase of the slip model. In the HEM model, the conservation equations for momentum and specific enthalpy of the two-phase mixture are formally identical with those of the single-phase flow. In the SM model, additional terms are included that take into account the so-called momentum-slip and enthalpy-slip between the phases. The momentum-slip term is treated implicitly, while the enthalpy-slip term is treated semi-implicitly. The rigorous sodium properties package used is based on work by Golden and Tokar [5]. The governing equations are those given in the COMMIX-2 document [2].

The problem was modeled in one-dimensional cylindrical coordinates using 52 nodes, each 4 cm high. The first 25 were heated and the next 25 unheated, followed by a one-node condenser and then an unheated node. Heating was prescribed as a constant heat flux. The problem was first run with an inlet velocity fixed at 2.7 m s^{-1} at an inlet temperature of 570°C. The initial velocity and temperature were the same. Although a flow bypass was used in the experiment, none was used in the simulation. After the steady-state was achieved, the inlet flow was decreased to 2.5 m s^{-1} over 100 time steps. Fixed time steps of 0.01 and 0.1 s were used.

In spite of modeling efforts, the numerics became unstable very soon after boiling was initiated. This was surprising and disappointing, in light of the relatively successful three-dimensional simulation of the much more complicated KFK 7-pin pump run-down sodium boiling experiments [6]. All three discretization options of the compressibility term $(\partial\rho_m/\partial t)_o^{n+1}$ contained in the b_o term of the combined continuity–momentum Poisson equation for pressure, given by

$$a_o\delta P_o^{n+1}-\sum_{\beta=1}^{6}a_\beta\delta P_\beta^{n+1}=b_o \tag{1}$$

were used. Index o refers to the center of a cell, while index β runs over the indices of the six neighboring cells in the three coordinate directions. In equation (1), δP^{n+1} is the pressure increment given by $\delta P^{n+1}=P^{n+1}-P^n$, where n represents a time discretization index. The three discretization options are

$$\left(\frac{\partial\rho_m}{\partial t}\right)_o^{n+1}=$$

$$\frac{\rho_{mo}^{k+1}-\rho_{mo}^{n}}{\Delta t}, \tag{2}$$

$$\left(\frac{\partial\rho_m}{\partial P}\right)_{h_{mo}}^{n}\left(\frac{P_o^{k+1}-P_o^{k}}{\Delta t}\right)+\frac{\rho_{mo}^{k}-\rho_{mo}^{n}}{\Delta t}, \quad \text{and} \tag{3}$$

$$\left(\frac{\partial\rho_m}{\partial P}\right)_{h_{mo}}^{n}\left(\frac{P_o^{k+1}-P_o^{n}}{\Delta t}\right)+\left(\frac{\partial\rho_m}{\partial h_m}\right)_{P_o}^{n}\left(\frac{h_{mo}^{k+1}-h_{mo}^{n}}{\Delta t}\right) \tag{4}$$

where k and $k+1$ refer to the iteration indices at time step level $n+1$.

The expressions for the derivatives of the coolant mixture density with respect to pressure and enthalpy may be found in Bridgman [7] and in the COMMIX-2 document [2]. Equation (4) proved to be the most stable discretization.

In all cases, the experimental two-phase flow multipliers—curve-fit as a function of X_{LM}, the Lockhart–Martinelli parameter—by Savatteri and Kottowski [1] were used. One slip correlation used in this study is given by the normalized relative slip velocity, $\tilde{\mathbf{V}}_{SL}^N$, defined as the ratio of the relative slip velocity to the mixture velocity component in the same coordinate

direction. With the reference to the z-coordinate direction, for example, we have

$$W_{SL}^{N} = \frac{W_{SL}}{w_m} = \frac{w_g - w_l}{w_m}. \quad (5)$$

The rationale for the form of this slip model is based upon the work of Ishii [8], who correlated the drift velocity, V_{gj}, as proportional to the volumetric flux, j. Rearranging and simplifying the correlation for churn-turbulent flow predicts that the relative velocity is of the order of the mixture velocity at atmospheric pressure. A second slip correlation used in this study is the relative slip velocity, given by

$$W_{SL} = w_g - w_l. \quad (6)$$

Similar definitions apply for the x- and y-coordinate directions.

The third slip correlation used in this study is the slip ratio, $\tilde{\mathbf{H}}$, given by (for the z-coordinate direction, for example)

$$H_z = \frac{w_g}{w_l} = \frac{w_m + (1-x)W_{SL}}{w_m - xW_{SL}} \quad (7)$$

where x is the thermodynamic quality. The three components of these two slip correlations are given as constants in the three coordinate directions.

The HEM model is obtained as a subcase of the Slip Model by setting $H_x = H_y = H_z = 1$ or by setting $U_{SL}^{N} = V_{SL}^{N} = W_{SL}^{N} = 0$. Most simulations were run with the slip ratio computed from an empirical fit of the volume fraction as a function of the Lockhart–Martinelli parameter [1]. The results became unstable when boiling was initiated. In an attempt to isolate the source of the instability, a normalized slip velocity $W_{SL}^{N} = 1$ was used, which implies that the relative slip is equal to the mixture velocity. In spite of this more physically correct model, the results were less stable. Simplified properties were also tried, on the assumption that the complicated rigorous properties might contain an error, but the instability persisted.

After repeated failures to successfully simulate what appears to be a trivial problem, a new strategy of modeling was adopted and a new, but similar, experiment was chosen to be simulated. This experiment is Test Case 1, used as a benchmark problem for the European Liquid Metal Boiling Working Group [3]. The experiments were undertaken in the same apparatus as described above; however, more data were available, such as the pressure drop deeper into the single-phase region and the location of the boiling inception point as a function of flow rate. Computations from other computer programs were also presented.

Using the previously described model, runs with an inlet velocity of 4 m s^{-1} and a temperature of 584°C also produced numerical instability. However, runs in the single-phase region were stable, and the computed pressure drop agreed well with the data (as shown at the top of Fig. 1) and with hand calculations given by

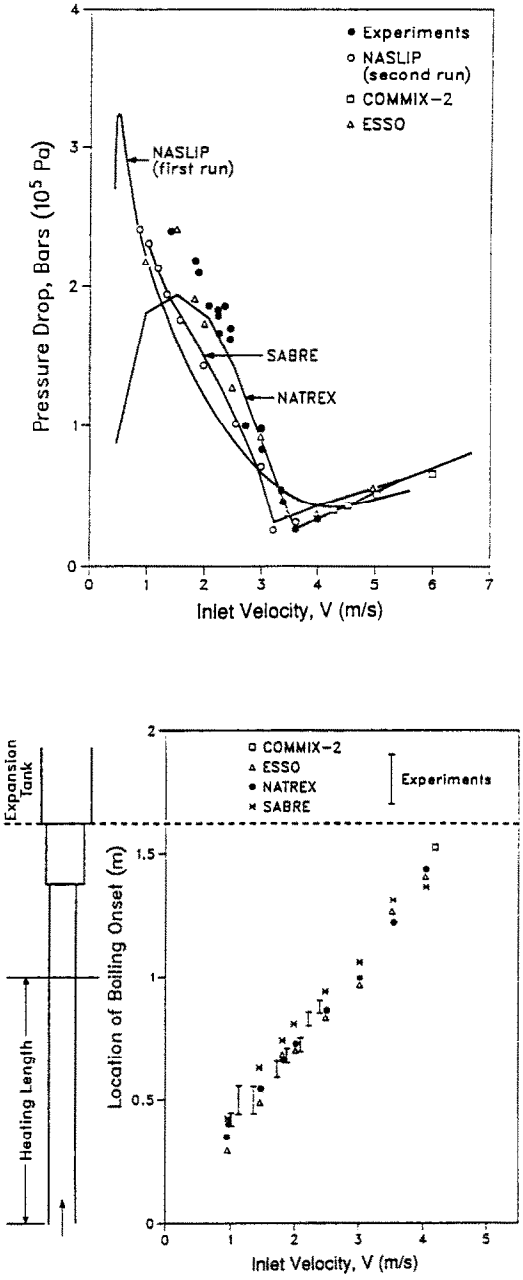

FIG. 1. Steady-state tubular tests—top: experimental and predicted pressure drops; bottom: comparisons of experimental and computed boiling point onset (modified from ref. [3]).

$$\frac{(-\Delta P)}{L} = \frac{f\rho w^2}{2D} \quad (8)$$

where

$$f = 0.3164\, Re^{-0.25}. \quad (8a)$$

Equation (8a) was used in all simulations reported

herein, except as noted. The computed pressure drop also agreed better with experimental results than any of the other computer codes (NASLIP, ESSO, SABRE, and NATREX) used to analyze the problem, as can be seen at the top of Fig. 1 [1].

The problem was remodeled and further simplified. One-dimensional Cartesian coordinates were used, and the prescribed heat flux boundary condition was replaced by a volumetric heat source in the fluid and a volumetric heat sink in the condenser to eliminate any problems possibly arising from heat transfer correlations. The new model also had 52.4 cm high nodes. This time, however, the first 5 nodes were unheated, the next 25 nodes contained the heat sources (1.249×10^6 kW m^{-3}), the next 15 nodes were unheated, and the next 6 nodes simulated the condenser, with a total heat sink equal to the heat source ($Q_{\text{SINK}} = -Q_{\text{SOURCE}} = 35.32$ kW) (5.21×10^6 kW m^{-3}); finally, there was 1 unheated node at the exit. No two-phase multipliers or slip were used, so the simulation corresponds to the HEM model with absolutely no empirical models.

In previous simulations, many nodes initiated boiling simultaneously; the flow was then adjusted until only a single node boiled. This time, the transient was initiated by turning on the heat source and sink in the heated and condenser sections, using an adiabatic single-phase steady-state initial condition. In this case, the flow is nearly steady when boiling begins. In fact, this was the alternative manner in which the lowest velocity, most unstable flow boiling experiments were performed by Savatteri and Kottowski [1].

This time a steady-state was achieved. As soon as boiling was initiated (in node 46), the number of iterations increased dramatically, from about seven to several hundred. By about 2 s into the transient, a new steady-state was achieved. The steady-state pressure profile is shown in Fig. 2 by the solid curve denoting 'old momentum flux'. A very large pressure drop, followed by a substantial recovery, occurs across the boiling region. We will refer to this as a pressure 'kink'.

There are several important observations to note about this simulation:

1. The pressure is *below* ambient pressure one node above the boiling node, and the shape of the pressure profile in the boiling region unexpectedly resembles a kink.
2. The two-phase velocity exceeds the HEM model's speed of sound, and the mass flux is greater than the corresponding HEM critical mass flux.
3. Decreasing the flow even a little bit further, such that the void fraction came closer to 1.0 or more than one node initiated boiling, caused an uncontrolled decrease in the pressure until it became negative, causing the instability noted in prior simulations.

These items will be addressed individually.

The fact that steady-state pressure drop in the two-phase region is greater than in the single-phase region

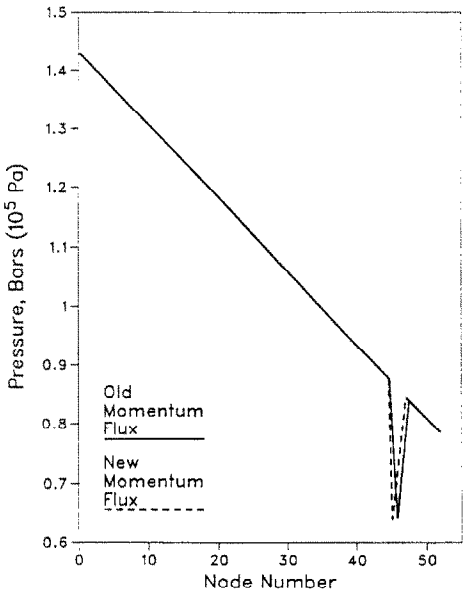

FIG. 2. Computed steady-state pressure profile at 4.2 m s^{-1} for the European Liquid Metal Boiling Working Group benchmark problem, test case 1.

makes sense. A steady-state momentum balance across the single- to two-phase region (suppressing frictional and gravity effects for clarity) yields the analytical solution:

$$\left.\begin{aligned}(\rho w)_{\text{lo}} &= (\rho w)_{2\phi} = \text{constant} = \rho w \\ P_{2\phi} - P_{\text{lo}} &= (\rho w)^2\left(\frac{1}{\rho_{\text{lo}}} - \frac{1}{\rho_{2\phi}}\right)\end{aligned}\right\}. \tag{9}$$

The subscripts lo and 2ϕ refer to 'liquid-only' and 'two-phase' conditions, respectively. Since $\rho_{2\phi}$ is less than ρ_{lo}, $P_{2\phi}$ must be less than P_{lo}, the pressure in the last single-phase liquid-only node. Also, since a steady-state exists, from continuity, the two-phase mixture velocity is greater than the liquid velocity because the density is less, causing the pressure to drop accordingly. However, a pressure below ambient level should be viewed with suspicion, although it is not considered to be an impossibility. The pressure should increase going from the two-phase region to the single-phase region, for the reasons discussed above.

Thus, the kink shown in Fig. 2 is at least qualitatively correct. Since the pressure drop in the experiment is measured across the entire heated region, it is possible that a part of the reason the experimental pressure drop increases after the inception of boiling is the decreased pressure in the boiling region. The other reason, of course, is that the two-phase mixture has a higher pressure drop. Yet another reason is discussed later.

Padilla and Rowe [9] noticed a kink and displaced pressure drop in their computed pressure profiles

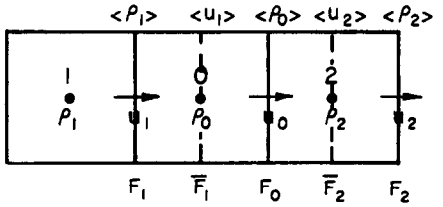

FIG. 3. COMMIX-2 nodalization scheme.

when large density changes occurred in steady-state boiling, and they reformulated the momentum–flux term. Thinking this to be the source of our stability problem, we changed the momentum–flux formulation in COMMIX-2. The following discussion explains the change.

Consider the steady one-dimensional momentum equation with zero gravity and equal area given by

$$\frac{\mathrm{d}}{\mathrm{d}x}(Fu)+\frac{\mathrm{d}P}{\mathrm{d}x}=0 \tag{10}$$

where $F=\rho u=$ constant.

Equation (10) may be integrated between the points 0 and 2, as shown in Fig. 3 as

$$\int_0^2 \frac{\mathrm{d}}{\mathrm{d}x}(Fu)\,\mathrm{d}x+\int_0^2 \frac{\mathrm{d}P}{\mathrm{d}x}\mathrm{d}x=\bar{F}_2\langle u_2\rangle -\bar{F}_1\langle u_1\rangle+P_2-P_0=0. \tag{11}$$

The brackets indicate that donor-cell differencing is being applied to u based on the sign of $\bar{F}$. The old formulation for the momentum fluxes $\bar{F}_1$ and $\bar{F}_2$ in COMMIX-2, defined at the edges of the dotted momentum cell as shown in Fig. 3, are given by

$$\left.\begin{aligned}\bar{F}_1&=\tfrac{1}{2}(F_1+F_0)\\ \bar{F}_2&=\tfrac{1}{2}(F_0+F_2)\end{aligned}\right\} \tag{11a}$$

where

$$\left.\begin{aligned}F_0&=\langle\rho_0\rangle u_0\\ F_1&=\langle\rho_1\rangle u_1 \text{ and}\\ F_2&=\langle\rho_2\rangle u_2\end{aligned}\right\}. \tag{11b}$$

For $u>0$, $\langle u_1\rangle=u_1$, $\langle u_2\rangle=u_0$; $\langle\rho_0\rangle=\rho_0$, $\langle\rho_1\rangle=\rho_1$, and $\langle\rho_2\rangle=\rho_2$. Solving for $-(P_2-P_0)$, equation (11) then becomes

$$-\Delta P_{\mathrm{acc}}=-(P_2-P_0)=\tfrac{1}{2}(\rho_0u_0+\rho_2u_2)(u_0)-\tfrac{1}{2}(\rho_1u_1+\rho_0u_0)u_1. \tag{12}$$

At steady-state, $\rho_0u_0=\rho_1u_1=\rho_2u_2=\rho u=$ constant, and therefore equation (12) may be expressed as

$$-(P_2-P_0)=(\rho u)(u_0-u_1)=(\rho u)\left(\frac{\rho u}{\rho_0}-\frac{\rho u}{\rho_1}\right)$$

or

$$-(P_2-P_0)=(\rho u)^2\left(\frac{1}{\rho_0}-\frac{1}{\rho_1}\right)=-\Delta P_{\mathrm{acc}}. \tag{13}$$

Equation (13) shows that the acceleration pressure drop does not occur where the density change occurs. If ρ_2 is much less than either ρ_0 or ρ_1, then the largest pressure drop does not occur between points 2 and 0. but is shifted a full node further downstream.

The modifications made are

$$\langle u_1\rangle=\langle\rho_1\rangle u_1/\rho_0=\begin{cases}\rho_1u_1/\rho_0, & \bar{F}_1>0\\ \rho_0u_0/\rho_0, & \bar{F}_1<0\end{cases} \tag{14a}$$

and

$$\langle u_2\rangle=\langle\rho_2\rangle u_2/\rho_2=\begin{cases}\rho_0u_0/\rho_2, & \bar{F}_2>0\\ \rho_2u_2/\rho_2, & \bar{F}_2<0\end{cases} \tag{14b}$$

$\bar{F}_1$ and $\bar{F}_2$ are unchanged in their formulation.

For $u>0$, we obtain

$$-(P_2-P_0)=(\rho u)^2\left(\frac{1}{\rho_2}-\frac{1}{\rho_0}\right). \tag{14c}$$

Now the pressure drop occurs where the density changes, which is the same as the analytical solution (equation (9)). When the simulation was rerun, all that changed was that the kink in the pressure profile was shifted upstream one node, as shown in Fig. 2 (as indicated by the curve 'new momentum flux') so that the large pressure change occurs where the density change occurs. The position of the boiling point inception is shown at the bottom of Fig. 1. As can be seen, its position agrees with the trend established by the data and the predictions from the other computer programs.

As a possible source of instability, the mass flux was checked against the critical mass flux for the HEM model. It was found that the HEM model's speed of sound and corresponding mass flux were greatly exceeded. The converged two-phase velocity was 10.6 m s^{-1}, while the mass flux was 3.49×10^3 kg m^{-2} s^{-1}. The HEM speed of sound at 10^5 Pa (1 bar) and zero quality is only slightly greater than 1 m s^{-1}, while the corresponding mass flux is only about 900 kg m^{-2} s^{-1}. In Fig. 4, the critical mass flux is plotted compared with sodium critical flow data [10]. As can be seen, at very low quality, the HEM model's critical mass flux is well below the data. The mass flux for this experiment [3] is on the same order as the low (less than 0.005) quality data. At higher quality, the rates scatter around the HEM model's value. The converged quality for this simulation was 4×10^{-4}. Even though this is low, it corresponds to a volume fraction of 0.44; however, the corresponding HEM speed of sound is still equal to only about 2 m s^{-1}.

There is a fundamental problem which exists, one which presents a paradox. If the single-phase velocity is above the HEM model's speed of sound, at the very first iteration when boiling occurs, the velocity of the two-phase mixture will become supercritical. Dechok-

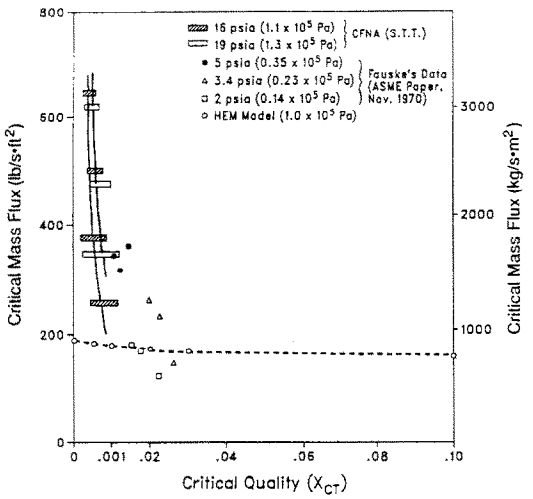

FIG. 4. Sodium critical flow data comparison (modified from ref. [10]).

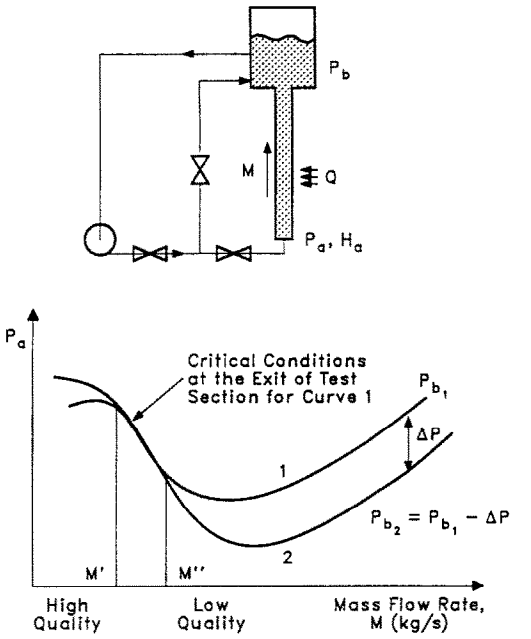

FIG. 5. Determination of critical flow rates on a forced convection boiling loop (modified from ref. [10]).

ing can then be caused in several ways: (1) the pressure can increase, causing the speed of sound to increase; (2) the quality can increase, which would also cause the speed of sound to increase; or (3) the flow can remain supersonic. The first possibility would result from the large volume of two-phase mixture formed from the liquid. However, the steady-state analysis shows that the pressure must *drop* in the transition from single- to two-phase mixture. The second possibility (increased quality) is indeed what happens, but in our case the converged mass flux still exceeded the HEM model's value. The last possibility may be a result of heating.

In any case, we are clearly dealing with a flow that is, in all likelihood, in a state we will refer to as critical flow boiling. This subject has not been studied very much, and its existence is not widely known: Costa and Charlety [10] seem to be the only ones to have carefully investigated the phenomenon. Figure 5 illustrates how Costa and Charlety test for critical flow boiling. Imagine two experimental runs (1 and 2) in which the downstream pressure P_b is reduced as indicated for a fixed heat flux, Q, and fixed inlet enthalpy (or temperature) h_a. In each run, the flow (indicated by M) is decreased, and the S-shaped pressure vs flow curve is experimentally produced. If the two curves 1 and 2 join as shown in Fig. 5, then by definition the flow is critical in the range M', M'', since the flow rate is independent of downstream conditions. The sodium forced-convection loop (CFNa) data obtained by Costa and Charlety in this manner are shown in Fig. 4, where they are compared with Fauske and Grolmes' critical flow data [11] and the computed HEM critical flow curve for 1.0×10^5 Pa (1 atm). From the data, it is clear that the flow becomes critical almost immediately after the inception of boiling and exists in the region where the pressure is rising with decreasing flow.

As a test of the COMMIX-2 code to achieve critical or choked flow, a simple problem was simulated that incorporates some analytical checks for correctness. The problem entails frictionally choked flow of an ideal diatomic gas, having a ratio of heat capacity at constant pressure to heat capacity at constant volume $C_p/C_v = k = 1.4$ and a molecular weight of 28, subjected to a decompression in a horizontal pipe. The properties of this gas are given by

$$\rho = \frac{P}{\bar{R}(T+273.15)} \tag{15}$$

and

$$\mathrm{d}h = C_p \mathrm{d}T \tag{16}$$

where T is temperature (°C), P is pressure (Pa), ρ is density (kg m^{-3}), $\bar{R} = 296.94$ Pa m^3 °C^{-1} kg^{-1}, $C_p = 1039.29$ J kg^{-1}, and h is enthalpy (J kg^{-1}). The viscosity is negligible, compared to the friction.

A run was made with the following conditions:

initial temperature = 196.75°C,
initial pressure $P = 1.51685 \times 10^7$ Pa,
decompression at one end to $P = 1.15118 \times 10^7$ Pa in 10^{-4} s, and
friction parameter $4fL/D = 0.1$ ($L = 3.75$ m, $f = 6.835 \times 10^{-5}$, $D = 0.01$ m).

The inlet temperature and pressure were maintained at the initial values. The pressure profiles at 2.5, 5 and 7 ms are plotted in the top of Fig. 6. The vertical lines represent the theoretical position of the head of the pressure wave for the case of zero friction. As can be

seen, the decompression wave with friction moves at about the right speed, and the wave form is smeared out. The bottom of Fig. 6 is a plot of the inlet and outlet velocity transients for this problem. The heavy solid and dashed lines up to about 300 m s^{-1} represent the analytical solution obtained from a wave diagram method of characteristics calculation using zero friction. The propagation rate calculated by COMMIX-2 agrees well with this solution, as do the values of the velocities.

The analytical solution given by equation (6-20) in Shapiro [12] was extended for nonunity Mach number at the exit of the pipe as

$$\frac{4fL}{D} = \frac{M_{out}^2 - M_{in}^2}{kM_{in}^2 M_{out}^2} + \frac{k+1}{2k} \ln \left[\frac{1 + \frac{(k-1)}{2} M_{out}^2}{1 + \left(\frac{k-1}{2}\right) M_{in}^2} \cdot \frac{M_{in}^2}{M_{out}^2} \right] \quad (17)$$

where M is the Mach number $= u/C$ (C is the local speed of sound). When $M_{out}^2 = 1$, equation (17) reduces to equation (6-20) in Shapiro [12]. The steady-state inlet mach number M_{in} was 0.8285 and the outlet mach number was 1.08, whereas an independent analytical calculation showed these values should be 0.77 and 0.994, respectively. The former two values do not allow equation (17) to balance, while the latter two do. This calculation indicates that even for this simple problem, the speed of sound is slightly exceeded with the code. The values of the flow may be incorrect because of the boundary-condition treatment and/or the momentum–flux treatment.

To prove the COMMIX-2 code is stable when the speed of sound is *not* exceeded, another simulation was performed. This was a one-dimensional representation of a 19-pin electrically heated steady-state test performed on the CFNa loop at Grenoble, France [13]. The conditions of the simulation were as follows:

inlet temperature = 400°C,
inlet velocity = 0.413 m s^{-1} (60 g s^{-1}), and
outlet pressure = 1.4×10^5 Pa.

The total power was 4.25×10^4 W. Twelve nodes were used in Cartesian coordinates. The first was 0.12 m high, and the rest were 0.1 m high. The first node was adiabatic, the middle six nodes had a volumetric heat source of 4.17×10^8 W m^{-3}, and the last five nodes were adiabatic. All nodes were 1.3×1.3 cm in cross section. The flow was chosen so boiling occurred at the end of the heated region (node 7).

The results are shown at the top of Fig. 7 for the case of slip ratio = 1.0 and two-phase friction multiplier = 1.0. The upper pressure profile (denoted by circles) is computed with the unmodified momentum flux, given by equations (11a) and (11b). This pressure profile shows that the largest pressure drop occurs between nodes 7 and 8, which is shifted downstream

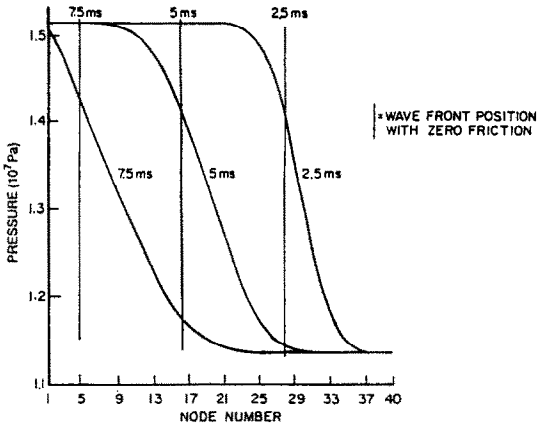

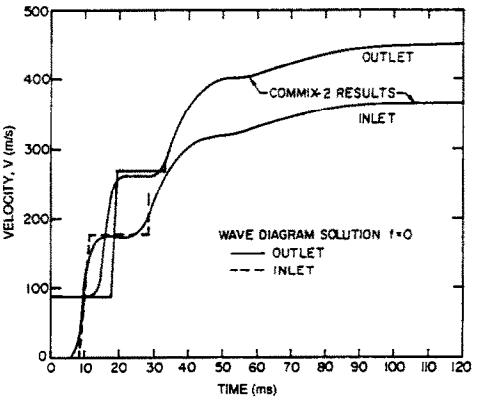

FIG. 6. Ideal gas decompression—top: pressure profiles at 2.5, 5 and 7.5 ms; bottom: computed inlet and outlet velocity transients. $4fL/D = 0.1$, initial speed of sound = 444 m s^{-1}.

of the location where the density changes the most (between nodes 6 and 7). Even though the void fraction, α_g, changes from 0 to 0.95 in a single node, and the density changes from 740 to 47 kg m^{-3}, the results are stable. The lower pressure profile is computed using the new momentum–flux formulation given by equations (14a) and (14b). This time, the largest pressure drop occurs where the density changes the most, as would be expected. Note that there is no kink in the pressure profile. These results compare quite closely with those of Schor and Todreas [14]. Although Padilla and Rowe [9] found that their execution time was reduced by 50% with the momentum–flux formulation changes, we found the opposite. The number of time steps needed for the solution to converge to a relative error of 10^{-5} increased from 58 to 84 using one iteration per time step. This simulation

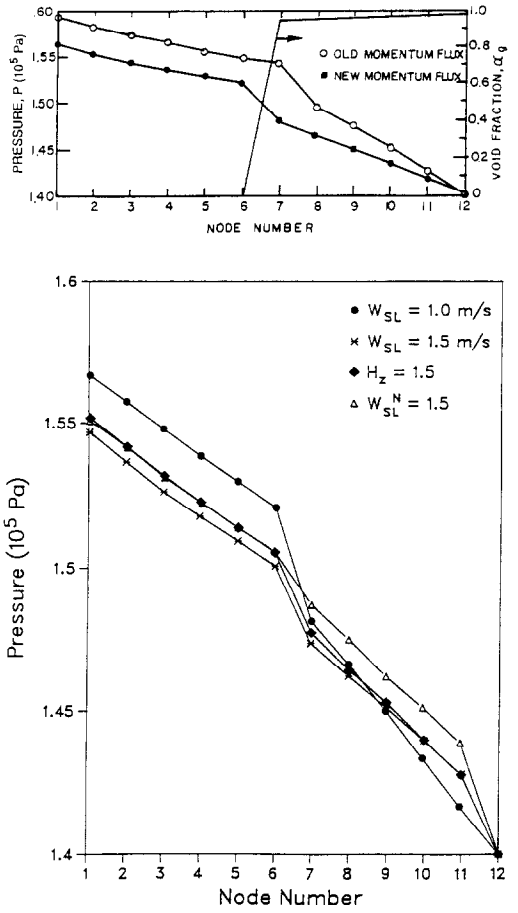

FIG. 7. One-dimensional model of Grenoble CFNa loop—top: comparison of old and new momentum-flux formulations for computed pressure profiles; bottom: effect of slip and two-phase flow multipliers on computed pressure profiles (ref. [13]).

was stable and the HEM model's speed of sound was never exceeded. The effect of slip models and the Lockhart–Martinelli two-phase multiplier was studied. The effect of slip lowered the pressure drop slightly, and the two-phase multiplier flattened the pressure profile somewhat in the two-phase region (as shown at the bottom of Fig. 7). Therefore, it is concluded that the various slip model correlations studied in this paper do not introduce the instability.

Another flow boiling simulation using high-pressure water was performed to demonstrate again that numerical stability results when the HEM model's speed of sound is not exceeded. Thom *et al.* [15] measured the void fraction in a steam–water mixture flowing in an electrically heated tube. Single-phase water was introduced at the inlet of the test section, and bulk or saturated boiling was present near the test section outlet.

The test section tube had a heated length of 1.524 m (5 ft) and an inside diameter of 9.754 mm (0.384 in.). Density measurements were made with a Thulium-170 gamma source, and these measurements were used to compute local void fractions. Density measurements were made every 4.45 cm (1.75 in.) between 0.273 m (10.75 in.) from the inlet and 0.139 m (5.5 in.) from the outlet.

One experiment (Test No. 12) was simulated with the COMMIX-2 code. The pressure for this run was 5.2724×10^6 Pa (764.7 psia), the uniform heat flux was 9.053×10^5 W m^{-2} (2.87×10^5 Btu ft^{-2} hr^{-1}), the mass flux was 9.53×10^2 kg m^{-2} s^{-1} (7.03×10^5 lb ft^{-2} hr^{-1}), and the inlet temperature was 225.56°C (438°F). This inlet temperature corresponds to an inlet subcooling of 41.7°C (75°F).

The 1.524 m (5 ft) heated test section was modeled in one dimension using 12 equally sized 0.127 m nodes. The analysis of this problem was performed with the steady-state option in COMMIX-2. With this technique, a very large time step is used, typically $\Delta t = 100$ s, which is about 1000-times larger than the transport time through a computational mesh. Steady-state was achieved in a minimum of only 11 time-step integrations (for no slip), using one iteration per time step. This required only about 1 s CPU time on an IBM 3033. The linearization for the density used both equations 3 and 4, which yielded essentially identical results. The water properties package is based on Agee's functional fits for density, enthalpy and temperature [16].

Several runs were performed to assess the slip models and the two-phase flow friction multipliers curve fit as a function of the Lockhart–Martinelli parameter, X_{LM}, by Savatteri and Kottowski, who found this approach suitable not only for water but also for sodium two-phase pressure drop [1]. The experimental void fraction data and the void fraction computed by the COMMIX-2 code are shown in Fig. 8 for three cases: slip ratios equal to 1 and 2, and

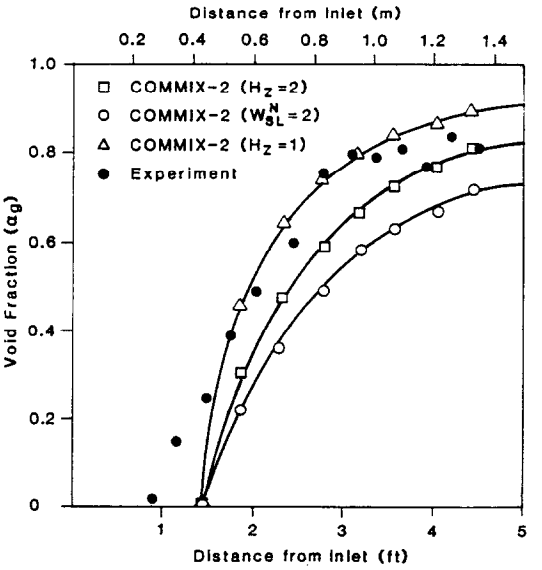

FIG. 8. Comparison of experimental and computed steady-state void fractions for test No. 12, Thom *et al.* (ref. [15]).

normalized slip velocity equal to 2. Clearly, the case of a slip ratio equaling 1 agrees with most of the data. The case of the slip ratio equal to 2 agrees with some of the data. The effect of the slip is quite pronounced, causing the void fraction to be lowered as the slip is increased. A normalized slip velocity equal to 2 produces slip ratios between 3 and 4. A more mechanistic slip ratio model may yield better results. The effect of the two-phase flow friction multiplier on the void profile for fixed slip ratio was negligible, but the pressure drop increase was considerable. All cases begin boiling later than the data indicate (about 0.4 m vs about 0.2 m), because thermodynamic equilibrium between the phases is assumed. Therefore, subcooled boiling is not predicted. Clearly, the data show that the subcooling persists only for a short distance (about 0.5 m), and then saturated boiling begins.

3. SOME POSSIBLE RESOLUTIONS

The steady-state analysis presented in the appendix shows very clearly, and conclusively, that a critical state exists for the calculation of the pressure gradient so that the velocity equals the HEM speed of sound, because the denominator on the right-hand-side of equation (A-11) becomes zero under this condition. Unless the compatibility condition is simultaneously satisfied (i.e. the numerator of equation (A-11) also becomes zero), the pressure gradient will be either difficult to accurately evaluate or impossible to compute at all. A possible resolution is to force the flow to be sonic when it exceeds the HEM model's speed of sound. This is usually done at breaks (i.e. system boundaries) where pressure is prescribed. When applied internally to the system, the solution of the momentum equation would have to be replaced by the compatibility condition given by the numerator on the right-hand-side of equation (A-11) being set to zero. Another resolution is to allow for a certain amount of thermodynamic nonequilibrium, such as a boiling delay relaxation time. This would, in effect, raise the speed of sound, especially at very low qualities.

It may be fruitless to seek a steady-state solution. The void fraction, flow, and pressure measurements of Savatteri and Kottowski indicate highly oscillatory conditions. Steady-state codes, such as ESSO [1], circumvent the problem of following this transient. Codes that solve a real or pseudo transient have to follow, to some extent, these oscillations. This probably requires much tighter coupling between the mass, momentum, and energy, perhaps by solving them not successively in the iteration cycle, but simultaneously.

The source of oscillations has been studied analytically and experimentally for condensing flow, which often accompanies flow boiling [17]. The Savatteri and Kottowski [1] and Costa and Charlety [10] experiments had condensers at the top. These were the simulations that presented the greatest difficulties. The experiments that simply have adiabatic sections with no condensation may be physically much less oscillatory and more amenable to steady-state computations. The flow bypass piping may also stabilize the system.

4. CONCLUSIONS

On the basis of the numerical simulations and analyses in this paper, the following major conclusions have been determined:

1. When the HEM model's speed of sound is not exceeded, no matter what slip model is used, stability results; when it is exceeded, none of the slip models can stabilize the results.
2. The numerical modeling of steady-state critical flow boiling using transient two-phase computer programs is an unresolved and major problem.
3. The treatment of the momentum flux term in the vicinity of large density changes has the effect of shifting the position where the pressure gradient change occurs, but this does not affect the numerical instability that occurs when the HEM speed of sound is exceeded at the inception of boiling.
4. Steady flow boiling is not steady at all and may at times be extremely violent, exhibiting large-amplitude flow, pressure, and void-fraction oscillations that are difficult to model numerically using transient computer models.
5. Additional pressure-profile data are needed for steady flow boiling in order to shed more light on the boiling process. Overall pressure-drop data are insufficient to understand conditions occurring in the transition region from single-phase to two-phase mixtures, and vice versa. Potentially large local pressure changes may occur and may escape detection.

Acknowledgments—This work was supported by the U.S. Department of Energy, under Contract W-31-109-Eng-38, and in part by the U.S. Nuclear Regulatory Commission through interagency agreement DOE 40-550-75 with the U.S. Department of Energy. Portions of this work were performed when the primary author was in the Analytical Thermal Hydraulics Research Program. The assistance and persistence of P. D. Esser in the preliminary calculations are appreciated.

REFERENCES

1. C. Savatteri and H. M. Kottowski, Two-phase flow liquid metal boiling characteristics. In *Heat Transfer in Nuclear Reactor Safety* (Edited by S. G. Bankoff and N. H. Afgan), Chapter 1.11, pp. 259–286. Hemisphere, Washington, D.C. (1982).
2. M. Bottoni (compiler), COMMIX-2: a three-dimensional transient computer program for thermal-hydraulic analysis of two-phase flows. Argonne National Laboratory Report ANL-85-47 [NUREG/CR-4371] (September 1985).
3. J. M. Seiler, Steady state boiling exercise. In *Proceedings of the Liquid Metal Boiling Working Group, Part II* (Edited by H. M. Kottowski and W. Peppler), pp. 1015 ff, held in Karlsruhe, West Germany (27–29 October 1982).
4. H. M. Domanus *et al.*, COMMIX-1A: a three-dimen-

sional transient single-phase computer code for thermal-hydraulic analysis of single and multicomponent systems, volume I: user's manual. Argonne National Laboratory Report ANL-82-25 [NUREG/CR-2896], ANL-82-25 (December 1983).
5. G. H. Golden and J. V. Tokar, Thermophysical properties of sodium, Argonne National Laboratory Report ANL-7323 (August 1967).
6. M. Bottoni *et al.*, Development of the three-dimensional, two-phase flow COMMIX-2-SM computer program, presented at XIth Liquid Metal Boiling Working Group Conf., Grenoble, France (23–26 October 1984).
7. P. W. Bridgman, *The Thermodynamics of Electrical Phenomena in Metals and a Condensed Collection of Thermodynamic Formulas*. Dover Press, New York (1961).
8. M. Ishii, One dimensional drift-flux model and constitutive equations for relative motion between phases in various two-phase flow regimes, Argonne National Laboratory Report ANL-77-47 (1977).
9. A. Padilla, Jr. and D. S. Rowe, A donor flow formulation for momentum flux differencing, *Trans. of the American Nuclear Society*, vol. 46, pp. 851–852. American Nuclear Society, La Grange Park, Illinois (1984).
10. J. Costa and P. Charlety, Critical-flow experiments in a forced convection boiling sodium loop. In *Progress in Heat and Mass Transfer* (Edited by O. E. Dwyer), pp. 429–439. Pergamon Press, Oxford (1973).
11. H. K. Fauske and M. A. Grolmes, Pressure drop forced convection flashing sodium, *Proc. Symposium on Liquid Metal Heat Transfer and Fluid Dynamics*. American Society of Mechanical Engineers, New York (November 1970).
12. A. H. Shapiro, *The Dynamics and Thermodynamics of Compressible Fluid Flow*, Vol. 1. Ronald Press, New York (1953).
13. G. Basque, D. Grand and B. Menant, Theoretical analysis and experimental evidence of three types of thermohydraulic incoherency in undisturbed cluster geometry, presented at IAEA Specialists' Meeting on Thermodynamics of Fast Breeder Reactor Fuel Subassemblies under Nominal and Non-nominal Operating Conditions, held in Karlsruhe, West Germany (1979).
14. A. L. Schor and N. E. Todreas, A four equation two-phase flow model for sodium boiling simulation of LMFBR fuel assemblies, MIT Energy Laboratory Report MIT-EL-82-039 (December 1982).
15. J. R. Thom *et al.*, Boiling in sub-cooled water during flow up heated tubes or annuli, *Proc. Inst. Mech. Engrs* **80(2C)**, 226–246 (1965–1966).
16. L. J. Agee, An analytical method of integrating the thermo-hydraulic conservation equations, *Nucl. Engng Design* **42**, 195–208 (1977).
17. G. L. Wedekind and B. L. Bhatt, An experimental and theoretical investigation into thermally governed transient flow surges in two-phases condensing flow, *J. Heat Transfer* **99(4)**, 561–567 (November 1977).

APPENDIX: PROOF THAT THE HEM MODEL'S SPEED OF SOUND IS A CRITICAL CONDITION FOR THE PRESSURE GRADIENT

Consider the steady-state one-dimensional constant area two-phase flow boiling equations in the form

Continuity

$$\frac{\partial}{\partial z}(\rho v) = 0. \tag{A-1}$$

Momentum

$$\frac{\partial}{\partial z}(\rho v v) + \frac{\partial P}{\partial z} = -\frac{f\rho v|v|}{2d_h} - \rho g. \tag{A-2}$$

Energy

$$\rho v \frac{\partial h}{\partial z} = v\frac{\partial P}{\partial z} + Q. \tag{A-3}$$

The subscript m for mixture has been suppressed.

The pressure gradient may be solved for from equation (A-2) and rearranged into the form

$$-\frac{\partial P}{\partial z} = \frac{fG|G|}{2d_h\rho} + G^2\frac{\partial}{\partial z}\left(\frac{1}{\rho}\right) + \rho g \tag{A-4}$$

where $G = \rho v = \text{constant}$.

Expansion of $\partial(1/\rho)/\partial z$ in terms of the thermodynamic or static quality, x, produces

$$\frac{\partial}{\partial z}\left(\frac{1}{\rho}\right) = x\left(\frac{\partial v_g}{\partial z} - \frac{\partial v_l}{\partial z}\right) + \frac{\partial v_l}{\partial z} + \left(\frac{1}{\rho_g} - \frac{1}{\rho_l}\right)\frac{\partial x}{\partial z} \tag{A-5}$$

where $v_g = 1/\rho_g$ and $v_l = 1/\rho_l$.

In the two-phase region, the phase densities are only a function of pressure. Use of this fact allows equations (A-4) and (A-5) to be combined and rewritten as

$$-\frac{\partial P}{\partial z} = \frac{\dfrac{fG|G|}{2d_h\rho} + G^2\left(\dfrac{1}{\rho_g} - \dfrac{1}{\rho_l}\right)\dfrac{\partial x}{\partial z} + \rho g}{1 - v^2/C_h^2} \tag{A-6}$$

where a speed of sound C_h^2 is defined as

$$C_h^{-2} = \rho\left(\frac{\alpha_g}{\rho_g C_g^2} + \frac{\alpha_l}{\rho_l C_l^2}\right). \tag{A-7}$$

This speed of sound is the homogeneous speed of sound at constant enthalpy. Since it is defined in terms of

$$C_g^{-2} = \frac{d\rho_g}{dP} \quad \text{and} \quad C_l^{-2} = \frac{d\rho_l}{dP} \tag{A-8}$$

it does not have a physical interpretation since it can become negative.

The derivative of quality, $\partial x/\partial z$, can be expressed in terms of enthalpy and pressure. Equation (A-6) may be rewritten in the equivalent form

$$\frac{\partial P}{\partial z} = \frac{\dfrac{fG|G|}{2d_h\rho} - G^2\left(\dfrac{\partial\rho}{\partial h}\right)_P\dfrac{dh}{\partial z} + \rho g}{1 - v^2/a_h^2} \tag{A-9}$$

where the HEM model's speed of sound at constant enthalpy is given by

$$a_h^2 = \left(\frac{\partial P}{\partial\rho}\right)_h. \tag{A-10}$$

Use of the energy equation, equation (A-3), allows us to write equation (A-9) in the final form

$$-\frac{\partial P}{\partial z} = \frac{\dfrac{fG|G|}{2d_h\rho} + \rho g + \dfrac{Q}{\rho}}{1 - v^2/a_s^2} \tag{A-11}$$

where the HEM model's speed of sound at constant entropy is given by

$$a_s^{-2} = \left(\frac{\partial\rho}{\partial P}\right)_S = a_h^{-2} + \frac{1}{\rho}\left(\frac{\partial\rho}{\partial h}\right)_P. \tag{A-12}$$

Clearly, from equation (A-11), when $v = a_s$, $\partial P/\partial z$ goes through a critical condition and the gradient of pressure can only remain finite if the numerator also goes to zero. This is the compatibility condition.